Visible to Mid-Infrared Photodetector Based on Black Phosphorous-MoS_2 Van Der Waals Heterojunction

Qi Han, Yadong Jiang, Xianchao Liu, Chaoyi Zhang, and Jun Wang

***Abstract*—Van der Waals heterostructures of black phosphorous(BP) and Molybdenum Disulfide(MoS_2) is designed and evaluated for photodetection application from visible to mid-infrared wavelength up to 4.5 μm. The device possesses a low dark current less than 0.1 μA for short wavelength light. For visible and near infrared radiation, the contribution of heat and photo energy to current enhancement is analyzed. Dark current drift by joule heat and laser heat absorbed is observed in short waveband. The difference in response speed is believed to be a result of the competition of BP and MoS_2 photocurrent. Gate tunable response time and on-off ratio makes the device versatile in potential application. For mid infrared radiation, BP-MoS_2 heterojunction with a dedicated thickness tailoring of MoS_2 exhibits similar negative response as an intrinsic BP. The normalized detectivity is D^* of 2.02×10^8 $Jones$ for the 4.5 μm mid-infrared radiation. Elaborate reduction of the noise is conducted to get the time resolvable photo-response. A low bias is necessary for a time resolved photocurrent, reducing the flicker noise to an acceptable level.**

***Index Terms*—Black phosphorous, mid infrared, wide band photodetector, Van Der Waals heterojunction, Molybdenum Disulfide.**

I. Introduction

BLACK phosphorous [1] is a two dimensional material with layer dependent band gap, ranging from 0.3 eV to 1.8 eV for bulk form BP to monolayer BP [2]. The narrow direct band gap of bulk BP makes it suitable for infrared detection [3]. While in previous research, lock-in method used in mid infrared measurement enhances detection performance artificially and makes it difficult to find the intrinsic physical mechanism [4], [5]. Besides, intrinsic uniform BP lacks visible and near infrared sensitivity due to low light harvesting and instant local carrier recombination. Even if asymmetric structure is employed, the photodetection suffers from a large dark current [6]. Combining BP with another two-dimensional material is a solution for extending its effective spectrum. Several reports on BP-MoS_2 Van der Waals heterojunction confirms its feasibility [7], [8], [9]. Geonyeop Lee fabricated BP/MoS_2/BP heterojunction and got a gate tunable rectifying ratio [10]. Lei Ye extended the detection wavelength of BP/MoS_2 heterojunction to 1550 nm [11]. Thayer S. Walmsley uncovered that response time can be tuned through changing the gate voltage [12]. In this work, time resolvable photo-response of BP-MoS_2 heterojunction in visible, near infrared and mid infrared waveband is measured and compared with that of intrinsic BP.

Manuscript received 21 December 2022; revised 16 January 2023; accepted 29 January 2023. Date of publication 7 February 2023; date of current version 28 February 2023. This work was supported by the National Natural Science Foundation of China (NSFC) under Grants 61922022, 62175026, 62171094, and 62104026. *(Corresponding author: Jun Wang.)*

Qi Han, Xianchao Liu, and Chaoyi Zhang are with the School of Optoelectronic Science and Engineering, University of Electronic Science and Technology of China, Chengdu 610054, China (e-mail: hanqi.chengdian@foxmail.com; cy9151270@126.com; zhangcy1009@sina.com).

Yadong Jiang and Jun Wang are with the School of Optoelectronic Science and Engineering, University of Electronic Science and Technology of China, Chengdu 610054, China, and also with the State Key Laboratory of Electronic Thin Films and Integrated Devices, University of Electronic Science and Technology of China, Chengdu 610054, China (e-mail: jiangyd@uestc.edu.cn; wjun@uestc.edu.cn).

Digital Object Identifier 10.1109/JPHOT.2023.3241285

II. Materials and Methods

Au electrodes are deposited on 300 nm SiO_2/Si substrate with a 10 nm titanium moist layer. followed by black phosphorous transferring by use of universal two-dimensional material dry transfer method [13], [14]. Multilayers of BP, is first transferred above on electrode pad, leaving the other pad open. Then MoS_2 is transferred, connecting the BP to the other pad. Necessary measurement such IV curve is carried on single materials and their heterojunction. Multilayers of MoS_2 are purchased from Six-carbon technology, Shenzhen, China. The black phosphorous is purchased from Nanjing MuKe Nanotechnology Co., Ltd.

The photocurrent is collected by a PDA source meter. For visible and near infrared light, a laser with specified wavelength is used. The light spot differs one from another. For mid infrared radiation, a narrow band filter centered at 4.5 μm is placed before SiC black body for certain mid-infrared wavelength. The FWHM of the filter is around 500 nm. The spot size for these mid-infrared filtered light is estimated as 2 cm^2. And the time resolved response is recorded with a mechanical chopper.

III. Results and Discussion

Basic measurement setup is illustrated in Fig. 1(a) where the light source resembles lasers in visible to near infrared wavelength or a black body in with a filter in mid infrared wavelength. A metallographic microscope photograph of BP-MoS_2 heterojunction is in the inset of Fig. 1(a). Raman spectrum is measured to verify the overlying of BP [15] and MoS_2,also shown in the inset of Fig. 1(a).To fabricate this device, gold electrodes are patterned on SiO_2/Si substrate by ordinary ultraviolet lithography and thermal evaporation. BP exfoliated by scotch tape is transferred on the edge of the electrode, followed by the MoS_2 transfer connecting BP sheet and the other electrode. So the BP is covered by MoS_2 sheet. The thickness of MoS_2 is selected thin to decrease its radiation blocking influence to BP.

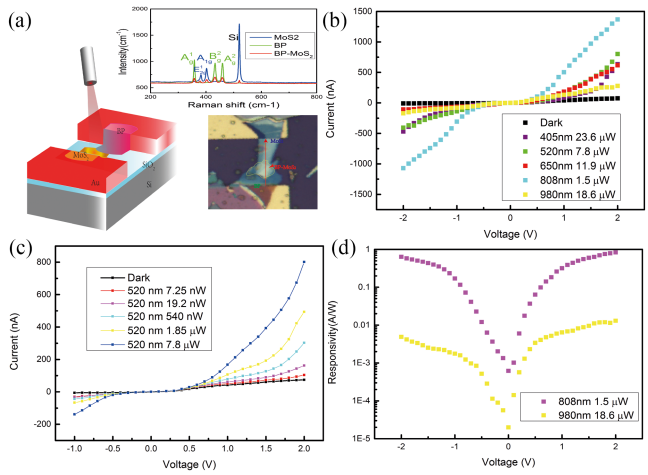

Fig. 1. (a) A schematic of device, Raman spectrum and photograph of BP-MoS_2 heterojunction. The Raman spectrum is denoted by its line color as the same in the metallographic microscope graph. (b) IV curve under lasers for visible and near-infrared radiation, (c) corresponding IV curve and of BP-MoS_2 heterojunction under 520 nm laser, (d) comparison of responsivity of the device for 808 nm and 980 nm calculated from IV curve.

The thickness of gold is 100 nm and the thickness of SiO_2 is 300 nm. Detailed thickness information of the heterojunction is measured using a profilometer. The thickness of gold electrode is known and subtracted from the total height data. As a result, the thickness of BP sheet is evaluated as 80 nm and the thickness of MoS_2 is around 6 nm.

IV curve of the Van Der Waals heterojunction is extracted for dark and bright condition, as shown in Fig. 1(b). Under dark condition, an apparent heterojunction behavior is observed. The current is -6.03 nA with a bias of -1 V and 41.4 nA with a positive bias of 1 V. This feature is similar to an ordinary p-n junction. While for a Van Der Waals junction, the gap at the interface needs modelling in a more subtle manner. Lee et al. modeled similar WSe_2/MoS_2 Van Der Waals heterojunction using traditional drift-diffusion equation with a phenomenological interlayer gap [16] and got a good accordance, which is enough for the analysis of BP/MoS_2 device. Comparing to single BP or MoS_2, the current is lower. For a BP sheet with a bias of 1 V, the resistance is several kilo-olms and for a MoS_2 sheet, the resistance is around 1 MΩ. While for our BP-MoS_2 device, the resistance is 24 MΩ in the same measurement environment. A steeper slope under small reverse bias indicates a part of charge stored in the junction. For a series circuit, voltage drops according to the ratio of resistance of each part. The voltage drop on pure BP or MoS_2 sheet is small, while most voltage is applied on the gap in the heterojunction.

There is a large difference in total current under laser incident for various wavelength as illustrated in Fig. 1(b). There is a changing of slope of the IV curve especially apparent for a 808 nm laser. Absolute value of total current rises rapidly after the bias cross 0.3 V to positive and -0.5 V to negative direction. leaving a flat zone is around zero bias. In this flat zone, even excess carriers are generated in a fast speed, the external electric field for carrier separation is not strong enough to overcome the barrier between BP and MoS_2. As a result, a relatively low external quantum efficiency (EQE) is recorded. By applying a high bias, the barrier is overcome. Then a combination of photoconductor and photo voltage effect appears. The thorough mechanism is hard to get. But when positive biased, the device behaves more like a photoconductor. The feature can be more apparent with a close look on the photocurrent for 405 nm and 520 nm lasers. When the Van Der Waals heterojunction is positive biased, the majority carriers in the BP or MoS_2 are accumulated near the interface of the junction. The excess carriers generated by incident radiation are swept by the electric field. They must cross the space between the BP and MoS_2 to make contribution to total current. Drawing from the experiment, the probability for the carriers leaping turns high when the bias is larger than 0.3 V.

To dismantle the photocurrent, the case of 520 nm radiation is taken as an example, illustrated in Fig. 1(c). A series of power is adopted for incident light. When positively biased, the photocurrent rises smoothly and responsivity decreases accordingly as the power increases. The photocurrent for a 19.2 nW is 13.2 nA under a bias of 1 V, yielding a responsivity of 0.69 A/W. And we get a photocurrent of 31 nA for an incident light power of 540 nW and a responsivity of 57 mA/W.

The photo-response is in expectation for visible wavelength. While if the laser wavelength is turned to near infrared, the responsivity changes a lot, as plotted in Fig. 1(d) in logarithmic coordinates. The bandgap of bulk MoS_2 is reported to be 1.2 eV [17]. That is, the absorption edge is 1033 nm. For the incident light with longer wavelength, intraband absorption of MoS_2 and the influence of BP would be complex. Experimentally, we get a responsivity of 0.9 A/W for a 808 nm and 0.01 mA/W for a 980 nm laser with a bias of 2 V. However, the responsivity directly evaluated from IV curve may be overestimated because heat absorbed by the device and joule heat cannot be released enough and they can make contributions to the total current. To discuss the photo-response mechanism in depth, time dependent current is measured.

Time resolvable photocurrent is shown in Fig. 2. More information of the BP-MoS_2 heterojunction can be clarified. The photosensitive mechanism of photodetectors are usually classified into two types, i.e., photo-electronic and photo-thermal effect. These two mechanism coexist in our BP-MoS_2 photodetector. The thermal effect is contributed both by the joule heat and the incident laser absorption. In the Fig. 2(a), the drift of dark current is due to the joule heat plus 405 nm laser energy absorbed. The baseline of photocurrent keeps steady if the bias is lower than 0.5 V, as shown in Fig. 2(a) for the 405 nm case. With a bias of 1 V, the dark current starts to grow as time passes. The dark current is 40 nA when the measurement is initially conducted. While the time is larger than 15 s, the dark current is 65 nA. After the light is turned off, the dark current then starts falling.

We can clarify the joule heat from laser power induced heat through varying the laser attributes. In Fig. 2(c), the total current of the device is measured under 808 nm for different incident power with a bias of 1 V. The power density of the laser for the case of 7430 nW is the same as that of 405 nm case in Fig. 2(a). The baseline in Fig. 2(c) keeps constant, meaning that joule heat plus the 808 nm laser energy absorbed by the device cannot

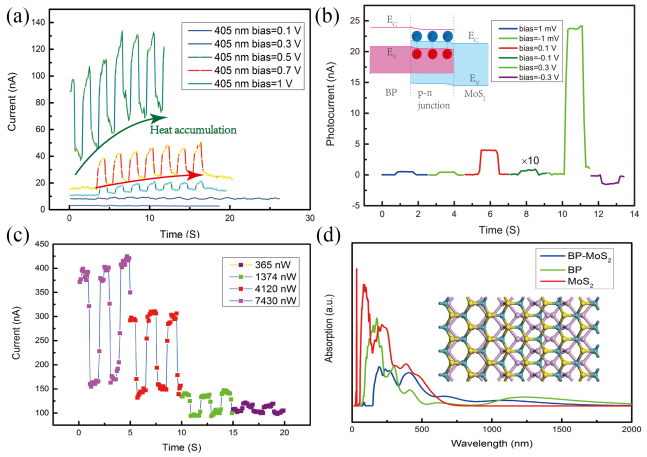

Fig. 2. Photocurrent of BP-MoS_2 under incident light ranging from 405 nm to 980 nm. (a) photocurrent under 405 nm with a series of bias with a rising dark current, (b) photocurrent under 650 nm illumination for different bias voltage, (c) photocurrent under 808 nm laser for different power. (d) spectrum of the BP-MoS_2 device modeled by first-principle method.

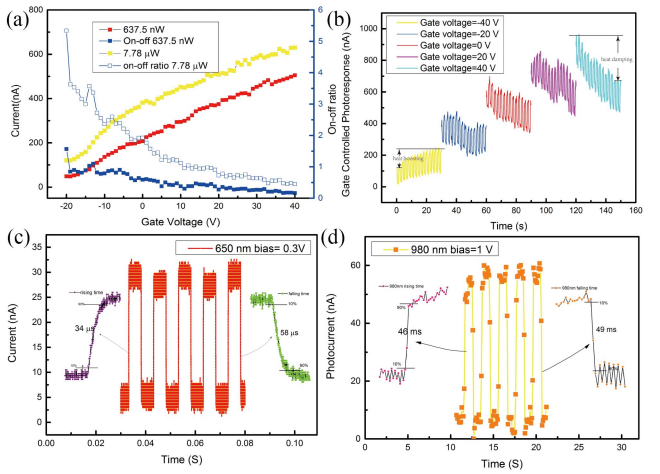

Fig. 3. Gate tunable BP-MoS_2 heterostructure response speed. (a) Transfer characteristic curve under 650 nm laser, (b) photocurrent speed under 980 nm laser, (c) gate tunable photocurrent under 650 nm laser, (d) response speed for different gate voltage.

induce the total current increasing with time. As a conclusion, the drift of dark current is mainly due to the 405 nm laser energy absorbed in the Fig. 2(a). This can be verified through absorption coefficient modelling of the device. The absorption spectrum modeled by first-principle is shown in Fig. 2(d). In the short waveband, the heterojunction absorption coefficient is much higher than other cases.

An illustration of photocurrent under 650 nm laser with a bias ranging from -0.3 V to 0.3 V is shown in Fig. 2(b). The dark current keeps constant thorough the measurement process. At a zero bias, holes in black phosphorus electrons in MoS_2 near the interface tends to diffuse to each other, leaving a built-in electric field in individual material. This process is like the traditional p-n junction except that a phenomenological interlayer should be introduced to model the quantum tunneling effect [16]. At a reverse bias, holes in black phosphorus and electrons in MoS_2 near the interface tends to be depleted, leaving a stronger built-in electric field. When the incident light impinges on the junction, the excess carriers generated are swept by the built-in electric field. The additional current due to the drift effect of built-in field can be denoted as I_{pv}. The total photocurrent I_{total} consists of photoconductivity part I_{ph} and I_{pv}. I_{pv} keeps its sign despite the direction of the bias, while I_{ph} turns negative with a negative bias and its absolute value magnitude is controlled by the magnitude of the lateral electric field, which is dominated by the external bias. If a little negative bias is applied such that $|I_{pv}|>|I_{ph}|$, the total photocurrent $I_{total} = I_{pv} - |I_{ph}|$ is still positive. However, the total photocurrent $I_{total} = I_{ph} + I_{pv}$ changes to negative if the magnitude of the applied negative bias is large enough. In Fig. 2(b), this is the case of a bias of -0.1 V. If the negative bias is set to -0.3 V, the photoconductivity effect dominates the photocurrent and we get a photocurrent of -2 μA.

The photocurrent for a 808 nm is plotted in Fig. 2(c). In this setup, a relatively long time of light exposure is performed before sampling until the dark current is almost flat. The thermal contribution to the photocurrent can be 150 nA, one third of the total photocurrent for the 7.43 μW case. A first-principle method modeling for the optical spectrum of BP-MoS_2 heterojunction is performed and the result is in the inset of Fig. 2(d). The space group of MoS_2 is R3M and the base vector is $a = b = 3.16$ $\dot{A}$, $c = 18.41$ $\dot{A}$. The space group of black phosphorus is Cmca and the base vector is $a = 3.31$ $\dot{A}$, $b = 10.5$ $\dot{A}$, $c = 4.38$ $\dot{A}$. The sudden decline of absorptance could cause the photo-electronic contribution of photocurrent less important in near infrared.

The BP-MoS_2 heterojunction is gate tunable [12], [19]. In our experiment, response time and on-off ratio can be tuned obviously as shown in Fig. 3. To analyze the response, a combination of gate voltage and bias voltage is applied on the device. When a large bias is induced, the excess electrons and holes are drifted by the applied voltage, then the response speed increases. The relationship of drain current and gate voltage shown in Fig. 3(a) proves that the BP-MoS_2 heterojunction behaves like a n type semiconductor, the majority carrier is electron. With a negative gate voltage, the electrons are expelled from the channel, so the number of the total carriers decreases accordingly. Then an incident light induced excess carriers can play a dominant role in current contribution. As a result, a relatively high on-off ratio is achieved in this condition.

The photocurrent is constantly evaluated with a laser power ranging from 1.12 nW to 7.78 μW, gate voltage ranging from -20 V to 40 V. As shown in Fig. 3(a), the dark current and photocurrent increase when the gate voltage is swept from -20 V to 40 V. At the bottom left corner of Fig. 3(a), a minimum of dark current is got. In this setup, the dark current is 1.75 nA and the corresponding total current under 11.9 μW incident light is 117 nA, yielding an on-off ratio of 66.9. When the gate voltage is swept to 40 V, the dark current increases to 800 nA and the photocurrent is 200 nA, yielding an on-off ratio of 1.25. Fig. 3(b) shows an overall photocurrent with varying the gate voltage, keeping a bias of 3 V. The magnitude of photocurrent keeps smooth among different gate voltage cases. With a negative gate voltage, the photocurrent can keep steady. But as the gate voltage

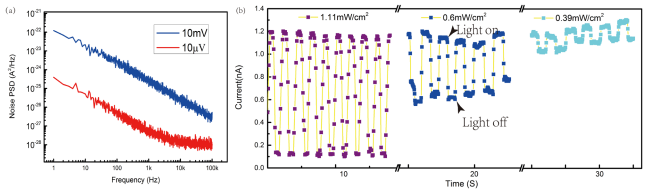

Fig. 4. Mid-infrared photocurrent of BP-MoS_2 heterojunction. (a) power density of noise for the BP-MoS_2 heterojunction, (b) a negative photocurrent under 4.5 μm radiation.

increases, the photocurrent drops as time passes. Combined with the experiment and conclusion in Fig. 2, along with the intrinsic feature reported in reference, a heat dissipation induced photocurrent decrease is inferred. There is a decay of total current with a large time constant.

The next interesting feature of the BP-MoS_2 heterojunction is the speed of the photocurrent. With the speed of the device determined, the normalized detectivity can be estimated. The typical response speed under 650 nm is relatively fast, shown in Fig. 3(c). The rise time is 34 μs and the falling time is 58 μs. The response speed for 980 nm laser is shown in Fig. 3(d). The rising time is 46 ms and the falling time is 49 ms. The incident light processes a switching speed fast enough through a calibrating work using a InGaAs commercial photodetector.

With the noise estimation approach we can calculate the detectivity for our heterojunction. The radiation power on the device is 59 nW and the photocurrent is 25 nA, thus the responsivity is 0.43 A/W. For the sampling rate could be low, we take a conservative mathematical analog rather than making Fourier transform to the signal [20]. The bandwidth is estimated thorough the equation $1/(\eta(t_r + t_f))$, where t_r and t_f resembles the rising time and falling time and η is an phenomenological coefficient. The rms noise is evaluated from moving average method for visible and near infrared wavelength. Then we can calculate the noise equivalent power(NEP) as $NEP = \frac{PSD}{R} = 6.97 \times 10^{-14}\ W \cdot Hz^{-1/2}$ and the corresponding normalized detectivity $D_1^* = A^{\frac{1}{2}}/NEP = 1.45 \times 10^{10}\ Jones$ [21]. The low detectivity here is because that we use high incident light and a low bias.

With the same experiment condition for 650 nm, a lower incident light power gives a better vision of NEP. If the incident light is switched to 3.57 nW, the photocurrent is around 7 nA. Estimation of responsivity gives 1.96 A/W and detectivity is $6.6 \times 10^{10}\ Jones$.

The noise of the BP-MoS_2 heterojunction is mainly located in low frequency range, as shown in Fig. 4(a).The main source of this noise is flicker noise. Actually, this is also true for a polysilicon resistor [22], MOSFET [23], [24] and many other systems [25]. However, with correlated double sampling (CDS) technique [26], low frequency noise can be reduced effectively. And this may be the reason of the appearance of the I_{Dark} dependent version of normalized detectivity. But in the scope of pure photodetector without discussing the read-out circuit, the normalized detectivity D$*$ or NEP considering the flickering noise is proper to estimate the performance of the device.

TABLE I
A SUMMARY OF BP/MoS_2 HETEROJUNCTION PHOTODETECTORS

Material/ ref	wavelength	Detectivity(Jones)	response time
BP/MoS_2[28]	365 nm to 660 nm	6.5×10^9	$> 10\ s$
BP/MoS_2[11]	532 nm 1.55 μm	3.1×10^{11} 2.13×10^9	15 μs
BP/MoS_2[9]	1.3 μm	~	~
BP/MoS_2[12]	650 nm, 1000 nm	~	13 μs
BP/MoS_2[29]	582 nm	~	$< 1\ s$
BP/MoS_2/BP [7]	633 nm	~	not stated
BP/MoS_2 (This work)	650 nm 808 nm 4.5 μm	6.6×10^{10} 1.1×10^9 2.02×10^8	~50 μs(visible) ~50 ms(infrared)

The photocurrent for mid infrared is in Fig. 4. Here a negative photo-response can be time resolvable. The incident light serves as heater and the black phosphorous sheet presents its metallicity. A dark current of ~1.2 nA is set for the BP-MoS_2 heterojunction and the photocurrent is approximately equally in value but opposite in direction, shown in Fig. 4(b). If the incident radiation is set to 1.11 mW/cm^2, the photocurrent is 1.2 nA. The radiation on the device is calculated to be 6.9 nW based on its area. The power spectral density of noise is extracted using a pwlech algorithm. It is a general spectral estimation utilizing fast Fourier transform. The result is in illustrated in Fig. 4(a). The rms noise is evaluated by integrating directly the power of signal density (PSD) over frequency bandwidth and taking the square root of the integrating result. As a result, the NEP is evaluated as $NEP = 8.2$ pW , the corresponding D^* is $2.02 \times 10^8\ Jones$. A total current falls around zero. We restricts bias low to decrease flicker noise, as the flicker noise can varies in order of magnitude with bias. In fact, time resolvable photocurrent cannot be extracted if a large dark current is present for both black phosphorous or BP-MoS_2 devices.

In Fig. 4(b), the relationship of mid-infrared photocurrent and the incident power for 4.5 μm light is shown. The photocurrent is negative. As the incident power is increased, it takes longer to reach the maximum photocurrent. The total current get saturable to around zero, and thorough mechanism requires more exploration.

Referring to a recent overview of black phosphorus based photodetectors [27] and some related works, a summary of photodetector based on BP/MoS_2 Van Der Waals heterojunction and other similar structures is listed in Table I. Most of them focus on the visible to near-infrared wavelength. The response time in ref [11] and ref [12] is 15 μs and 13 μs, faster than that of this work. Our device provides a overall estimation of BP/MoS_2 Van Der Waals heterojunction in a wide waveband.

IV. Conclusion

Heterostructures of black phosphorous(BP) and Molybdenum Disulfide(MoS_2) can be used for photodetection from visible to mid-infrared wavelength up to 4.5 μm. The device possesses a low dark current less than 0.1 μA for short wavelength light. The responsivity under a 520 nm is 0.69 A/W and the detectivity for a typical 650 nm laser is 6.6×10^{10} $Jones$. The competition of photo-electronic and photo-thermal mechanism of photodetectors is account for the response speed difference for a visible light and near infrared radiation. The heterojunction is gate tunable, so the on-off ratio can be adjustable. Photon injection and joule heat can make hybrid enhancement on the photocurrent. Time resolvable photocurrent for mid-infrared radiation is achieved. A responsivity of 2.2 mA/W and a D^* of 2.02×10^8 $Jones$ is recorded for 4.5 μm md-infrared radiation. The phenomena and theory could be beneficial for the designing of photodetectors based on two-dimensional Van Der Waals heterojunction.

References

[1] R. W. Keyes, "The electrical properties of black phosphorus," *Phys. Rev.,* vol. 92, no. 3, 1953, Art. no. 580.

[2] A. Castellanos-Gomez et al., "Isolation and characterization of few-layer black phosphorus," *2-D Mater.*, vol. 1, no. 2, 2014, Art. no. 025001.

[3] L. Huang et al., "Waveguide-integrated black phosphorus photodetector for mid-infrared applications," *ACS Nano,* vol. 13, no. 1, pp. 913–921, 2018.

[4] Q. Guo et al., "Black phosphorus mid-infrared photodetectors with high gain," *Nano Lett.*, vol. 16, no. 7, pp. 4648–4655, 2016.

[5] X. Chen et al., "Widely tunable black phosphorus mid-infrared photodetector," *Nature Commun.,* vol. 8, no. 1, 2017, Art. no. 1672.

[6] Q. Han, Y. Jiang, J. Han, X. Dong, and J. Gou, "Visible to mid-infrared waveband photodetector based on insulator capped asymmetry black phosphorous," *Front. Phys.,* vol. 9, 2021, Art. no. 710150.

[7] Y. Deng et al., "Black phosphorus–monolayer MoS_2 van der Waals heterojunction p–n diode," *ACS Nano,* vol. 8, no. 8, pp. 8292–8299, 2014.

[8] J. xu, J. Jia, S. Lai, J. Ju, and S. Lee, "Tunneling field effect transistor integrated with black phosphorus-MoS_2 junction and ion gel dielectric," *Appl. Phys. Lett.,* vol. 110, 2017, Art. no. 033103.

[9] X. Jiang et al., "Multifunctional black phosphorus/MoS_2 van der Waals heterojunction," *Nanophoton.*, vol. 9, no. 8, pp. 2487–2493, 2020.

[10] G. Lee, S. J. Pearton, F. Ren, and J. Kim, "Two-dimensionally layered p-black phosphorus/n-MoS_2/p-black phosphorus heterojunctions," *ACS Appl. Mater. Interfaces,* vol. 10, no. 12, pp. 10347–10352, 2018.

[11] L. Ye, H. Li, Z. Chen, and J. Xu, "Near-infrared photodetector based on MoS_2/black phosphorus heterojunction," *ACS Photon.*, vol. 3, no. 4, pp. 692–699, 2016.

[12] T. S. Walmsley, B. Chamlagain, U. Rijal, T. Wang, Z. Zhou, and Y.-Q. Xu, "Gate-tunable photoresponse time in black phosphorus–MoS_2 heterojunctions," *Adv. Opt. Mater.,* vol. 7, no. 5, 2019, Art. no. 1800832.

[13] Z. Huang et al., "High responsivity and fast UV-vis-short-wavelength IR photodetector based on Cd3As2/MoS2 heterojunction," *Nanotechnol.*, vol. 31, no. 6, 2019, Art. no. 064001.

[14] M. Buscema, M. Barkelid, V. Zwiller, H. S. J. van der Zant, G. A. Steele, and A. Castellanos-Gomez, "Large and tunable photothermoelectric effect in single-layer MoS_2," *Nano Lett.*, vol. 13, no. 2, pp. 358–363, 2013.

[15] S. Zhang et al., "Extraordinary photoluminescence and strong temperature/angle-dependent Raman responses in few-layer phosphorene," *ACS Nano,* vol. 8, no. 9, pp. 9590–9596, 2014.

[16] C.-H. Lee et al., "Atomically thin p–n junctions with van der Waals heterointerfaces," *Nature Nanotechnol.*, vol. 9, no. 9, pp. 676–681, 2014.

[17] M. Ye, D. Winslow, D. Zhang, R. Pandey, and Y. K. Yap, "Recent advancement on the optical properties of two-dimensional molybdenum disulfide (MoS_2) thin films," *Photonics*, vol. 2, no. 1, pp. 288–307, 2015.

[18] C.-H. Lee et al., "Atomically thin p–n junctions with van der Waals heterointerfaces," *Nature Nanotechnol.*, vol. 9, no. 9, pp. 676–681, 2014.

[19] F. Wu et al., "Gate-tunable negative differential resistance behaviors in a hBN-encapsulated BP-MoS_2 heterojunction," *ACS Appl. Mater. Interfaces*, vol. 13, no. 22, pp. 26161–26169, 2021.

[20] Y. Chen, S. Williamson, T. Brock, F. W. Smith, and A. R. Calawa, "375-GHz-bandwidth photoconductive detector," *Appl. Phys. Lett.*, vol. 59, no. 16, pp. 1984–1986, 1991.

[21] P. G. L. Datskos and V. Nickolay, "Detectors-figures of merit," *Encyclopedia Opt. Eng.,* vol. 349, no. 57, 2003.

[22] W. Pflanzl and E. Seebacher, "1/f noise temperature behaviour of poly resistors," in *Proc. 19th Int. Conf. Mixed Des. Integr. Circuits Syst.*, Warsaw, Poland, 2012, pp. 297–299.

[23] I. A. Young, "Analog mixed-signal circuits in advanced nano-scale CMOS technology for microprocessors and SoCs," in *Proc. Eur. Conf. Solid-State Circuits*, 2010, pp. 61–70,.

[24] C. H. Jan et al., "RF CMOS technology scaling in high-k/metal gate era for RF SoC (system-on-chip) applications," in *Proc. Int. Electron Devices Meeting*, 2010, pp. 27.2.1–27.2.4.

[25] M. S. Keshner, "1/f noise," *Proc. IEEE,* vol. 70, no. 3, pp. 212–218, Mar. 1982.

[26] M. H. White, D. R. Lampe, F. C. Blaha, and I. A. Mack, "Characterization of surface channel CCD image arrays at low light levels," *IEEE J. Solid-State Circuits,* vol. 9, no. 1, pp. 1–12, Feb. 1974.

[27] N. Deng et al., "Black phosphorus junctions and their electrical and optoelectronic applications," *J. Semicond.,* vol. 42, no. 8, 2021, Art. no. 081001.

[28] V. Krishnamurthi, M. X. Low, S. Kuriakose, S. Sriram, M. Bhaskaran, and S. Walia, "Black phosphorus nanoflakes vertically stacked on MoS_2 nanoflakes as heterostructures for photodetection," *ACS Appl. Nano Mater.,* vol. 4, no. 7, pp. 6928–6935, 2021.

[29] S. Zheng et al., "Acoustically enhanced photodetection by a black phosphorus-MoS_2 van der Waals heterojunction p-n diode," *Nanoscale,* vol. 10, no. 21, pp. 10148–10153, 2018.